Strojniški vestnik - Journal of Mechanical Engineering 51(2005)1, 13-27
UDK - UDC 532.528:004.94
Izvirni znanstveni članek - Original scientific paper (1.01)

Časovno odvisna simulacija, vizualizacija in meritve kavitacije z metodo PIV-LIF na različnih osamljenih profilih

Transient simulation, visualization and PIV-LIF measurements of the cavitation on different hydrofoil configurations

Matevž Dular - Rudolf Bachert - Brane Širok - Bernd Stoffel

Prispevek obravnava numerično in preizkusno študijo kavitirajočega toka okrog različnih osamljenih profilov. Za simulacijo neustaljenega toka je bil uporabljen programski paket Fluent. Dvofazni tok smo opisali z vpeljavo homogenega toka mešanice. Za popis nastanka in kolapsa kavitacijskega oblaka je bil uporabljen kavitacijski model, utemeljen na poenostavljeni Rayleigh-Plessetovi enačbi dinamike mehurčka. Narejene so bile trirazsežne simulacije kavitirajočega toka v različnih razmerah za dva osamljena profila.

Za dva profila smo posneli slike kavitacijskih struktur v različnih razmerah. Za določitev hitrostnega polja zunaj in znotraj kavitacijskega oblaka smo uporabili metodo PIV-LIF. Izmerili smo frekvence trganja kavitacijskega oblaka.

Numerično napovedane porazdelitve deleža pare in hitrostnega polja smo primerjali s preizkusnimi rezultati. Narejena je bila primerjava s preizkusi določenih in numerično napovedanih povprečnih dolžin kavitacijske strukture vzdolž profila. Primerjali smo tudi numerično napovedane in s preizkusi določene frekvence trganja kavitacijskega oblaka. V vseh primerih smo dobili dobro ujemanje med rezultati preizkusov in simulacij. Poleg tega je simulacija pravilno napovedala nastanek značilne podkvaste kavitacijske strukture.

(Ključne besede: kavitacija, dinamika tekočin, vizualizacija, metoda PIV-LIF)

This paper concerns a numerical and experimental study of cavitating flow around different single hydrofoils. The program package Fluent was used to calculate the unsteady flow, and the homogeneous flow principle was used to describe two-phase flow. The cavitation model based on a simplified Rayleigh-Plesset equation for bubble dynamics, was used to describe the appearance and collapse of a cavitation cloud. A 3D transient simulation of cavitating flow under different conditions for two hydrofoils was made.

Images of the vapour structures under different cavitation conditions for the two hydrofoils were acquired. A PIV–LIF method was used to obtain the velocity field inside and outside the vapour cavity. Measurements of the cavitation cloud shedding frequencies were made.

Numerically predicted distributions of the water vapour and the velocity field were compared with experimental results. The experimentally determined and numerically predicted mean cavity structure lengths along the hydrofoil were compared. Also, a comparison between the numerically predicted and the experimental cavitation cloud shedding frequencies was made. In all cases a good correlation between the experimental results and the numerical simulations was found. The simulation was also able to correctly predict the formation of typical "horseshoe" cavitation structures.

(Keywords: cavitation, compuatational fluid dynamics, visualization, particle image velocimetry (PIV))

0 UVOD

Pojav kavitacije v hidravličnih strojih vodi k problemom, kakor so vibracije, povečanje hidrodinamičnega upora, tlačni utripi, spremembe v

0 INTRODUCTION

The occurrence of cavitation in hydraulic machines leads to problems like vibration, an increase of hydrodynamic drag, pressure pulsation, changes

kinematiki toka, hrup in erozijo trdnih površin. Večina teh problemov je povezana s prehodnim obnašanjem kavitacijskih struktur [1], zato je študija neustaljenega obnašanja nujno potrebna za pravilno napoved prej omenjenih problemov.

V zadnjem desetletju je bilo razvitih mnogo metod za numerično simuliranje kavitirajočega toka. Večina teh metod obravnava dvofazni tok kot enofazni tok mešanice pare in vode. Uparjanje in kondenzacijo lahko modeliramo z različnimi izvornimi členi, ki so navadno izpeljani iz Rayleigh-Plessetove enačbe dinamike mehurčka ([2] do [5])) oziroma s tako imenovanim barotropičnim zakonom stanja, ki podaja odvisnost med gostoto mešanice pare in vode od lokalnega statičnega tlaka ([6] do [8]).

Prispevek obravnava preizkusno in numerično študijo neustaljenih pojavov kavitirajočega toka okoli dveh različnih profilov. Za določitev hitrostnega polja (zunaj in znotraj kavitacijskega oblaka) je bila uporabljena metoda vizualizacijske anemometrije (PIV) v kombinaciji s tehniko lasersko inducirane fluorescence (LIF). Trenutne slike parnih struktur smo posneli s kamero CCD. Za določitev robnih pogojev smo uporabili metodo laserske Dopplerjeve anemometrije (LDA), s katero smo določili hitrostni profil v ravnini pred profilom. Za trirazsežno nestacionarno simulacijo smo uporabili komercialni program za računalniško dinamiko tekočin Fluent 6.1.18. Za opis nestacionarnega obnašanja kavitacije, vključno s trganjem kavitacijskega oblaka, smo uporabili kavitacijski model, osnovan na enačbi dinamike mehurčka, ki je podrobneje opisan v [4].

1 POSTAVITEV PREIZKUSA

Preizkus je bil opravljen v kavitacijskem kanalu v Laboratoriju za turbinske in hidravlične stroje na Tehniški Univerzi v Darmstadtu.

Za preizkus smo uporabili dve preprosti geometrijski obliki. Osnovna geometrijska oblika je 50 mm širok, 107,9 mm dolg in 16 mm debel simetrični profil s polkrožnim vpadnim robom (PPVR - CLE) ter vzporednimi stenami. Z namenom, da bi dobili trirazsežne kavitacijske učinke, smo osnovno geometrijsko obliko spremenili tako, da smo vpadni rob profila odrezali pod kotom 25° in dobili profil z nesimetričnim vpadnim robom (PNVR - ALE) (sl. 1).

Profil je bil vstavljen v pravokotni testni odsek kavitacijskega kanala z zaprtim obtokom, kar omogoča spreminjanje tlaka sistema in posledično

in flow kinematics, noise and erosion of solid surfaces. Most of these problems are related to transient behaviour of cavitation structures [1]. Hence, a study of unsteady cavitation behaviour is essential for the correct prediction of these problems.

In the past decade a wide range of methods for the numerical simulation of cavitating flow were developed. Most of the studies treat the two-phase flow as a single vapour-liquid phase mixture flow. The evaporation and condensation can be modelled with different source terms that are usually derived from the Rayleigh-Plesset bubble dynamics equation ([2] to [5]) or by the so-called barotropic state law, which links the density of the vapour-liquid mixture to the local static pressure ([6] to [8]).

The paper discusses an experimental and numerical study of the unsteady phenomena of cavitating flow around two different hydrofoil configurations. The PIV (Particle Image Vecilometry) method combined with the LIF (Laser Induced Fluorescence) technique was used to determine the velocity field around the hydrofoil (outside and inside the vapour cavity). Instantaneous images of the vapour structures were recorded using a CCD camera. The LDA (Laser Doppler Anemometry) method was used to determine the boundary conditions by measuring the velocity in a plane in front of the hydrofoil. The commercial CFD (Computational Fluid Dynamics) code Fluent 6.1.18 was used for the 3D transient simulation. A cavitation model, based on bubble dynamics equations, described in [4], was used to describe the unsteady behaviour of the cavitation, including the shedding of the vapour structures.

1 EXPERIMENTAL SET-UP

The experiment was set up in a cavitation tunnel at the Laboratory for Turbomachinery and Fluid Power, Darmstadt University of Technology.

Two simple hydrofoils were used. The basic geometry is a 50-mm-wide, 107.9-mm-long and 16-mm-thick symmetrical hydrofoil with a circular leading edge and parallel walls (CLE – Circular Leading Edge hydrofoil). In order to obtain three-dimensional cavitation effects the basic geometry was modified by cutting the leading edge at an angle of 25 degrees (ALE – Asymmetric Leading Edge hydrofoil) (Fig. 1).

The hydrofoil was inserted into the rectangular test section of a cavitation tunnel with a closed circuit that made it possible to change the system pressure and consequently the cavitation number,

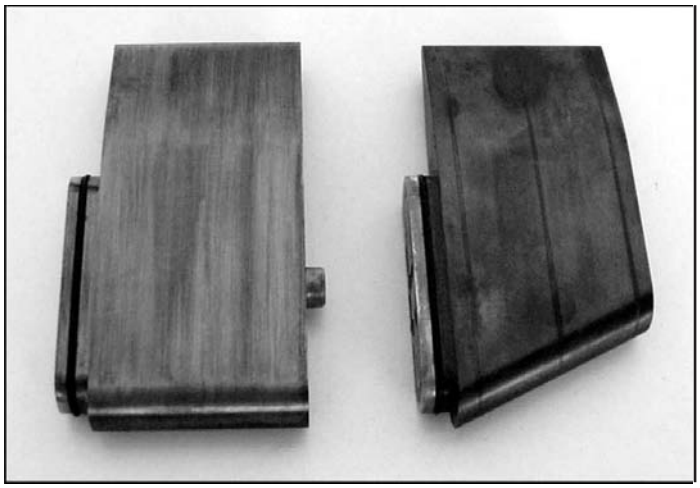

Sl. 1. *Osnovni profil – PPVR (levo) in spremenjeni– PNVR (desno)*
Fig. 1. *Basic – CLE (left) and modified – ALE hydrofoil (right)*

spreminjanje kavitacijskega števila, ki je definirano kot razlika med sistemskim tlakom in tlakom uparjanja (pri temperaturi sistema) deljena z dinamičnim tlakom:

which is defined as the difference between the system and the vapour pressure (at system temperature) divided by the dynamic pressure:

$$\sigma = \frac{p_\infty - p_v(T_\infty)}{\rho \cdot v^2 / 2} \quad (1).$$

Zmanjšanje kavitacijskega števila pomeni večjo verjetnost pojava kavitacije oziroma povečanje že prisotne kavitacije.

Hitrost v ravnini pred profilom je bila med preizkusom nespremenljiva $v = 13$ m/s (Re = 208000, glede na debelino profila). Obravnavali smo razviti kavitirajoči tok pri različnih vrednostih kavitacijskega števila (2,5, 2,3, 2,0) in 5° vpadnim kotom profila.

Decreasing the cavitation number results in a higher probability of cavitation occurrence or in an increase in the magnitude of the already-present cavitation.

The velocity in the reference plane in front of the hydrofoil was held constant at 13 m/s (Re = 208000 based on hydrofoil thickness). The developed cavitating flow at different values of the cavitation number (2.5, 2.3, 2.0) at a 5° angle of attack was observed.

2 PREIZKUSNO VREDNOTENJE KAVITIRAJOČEGA TOKA

Obravnavali smo obliko in dinamiko kavitacijskih struktur ter hitrostno polje v okolici profila. S kamero CCD smo posneli slike kavitirajočega toka z dveh pogledov (od zgoraj in od strani) (sl. 2).

Hitrostno polje smo določili z uporabo metode PIV-LIF. Za preizkus smo uporabili laser, dve kameri CCD, osebni računalnik in enoto za zbiranje in nadzor (sl. 3). Za osvetlitev smo uporabili navpično ravnino laserske svetlobe (laser Nd-YAG) z valovno dolžino 532 nm (zeleni spekter) debeline približno 1 mm. Položaj laserske ravnine je bil 5 mm od sprednje stene (kjer je profil najkrajši). Frekvenca zajemanja slik je bila približno 2 Hz.

2 EXPERIMENTAL EVALUATION OF THE CAVITATING FLOW

The shape and dynamics of the cavitation structures and the velocity field around the hydrofoil were investigated. The images of the cavitating flow were recorded with a CCD camera from the side and from the top (Fig. 2).

The velocity field was determined with the PIV-LIF method. The experimental setup (Fig. 3) consisted of a laser, 2 CCD cameras, a PC and an acquisition–control unit. A Nd-YAG laser vertical light sheet with a wavelength of 532 nm (green spectrum) and approximately 1 mm thick was used for the illumination. The position of the light sheet was 5 mm from the front wall (where the hydrofoil is the shortest). The frequency of the image capturing was approximately 2 Hz.

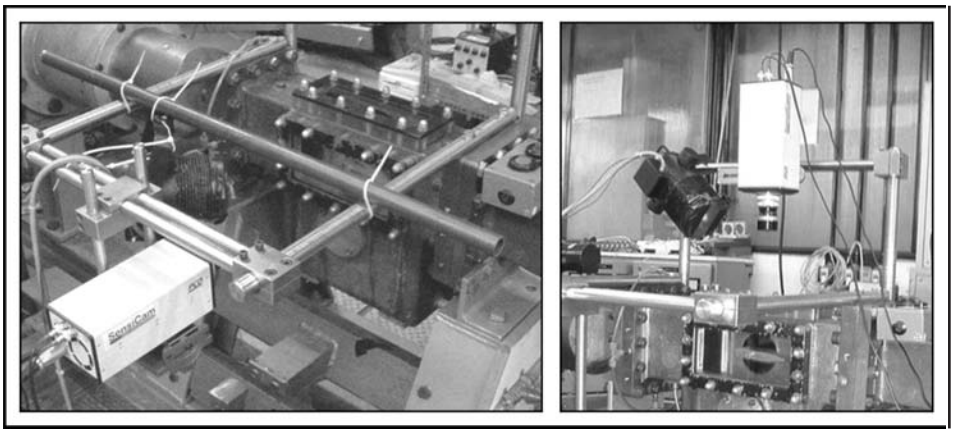

Sl. 2. *Postavitev kamere za snemanje slik s strani (levo) in od zgoraj (desno)*
Fig. 2. *Camera set up for recording the side-view (left) and top-view (right) images*

Problem uporabe metode PIV v kavitirajočem toku je, da kavitacijske strukture odbijajo preveč svetlobe. Tako določitev hitrostnega polja znotraj kavitacijskih struktur ni mogoča. Da bi dobili informacije o hitrostnem polju znotraj kavitacijskih struktur, smo uporabili razmeroma novo tehniko, pri kateri združimo metodo PIV z metodo LIF (glej tudi [10]). Za zrno smo vodi dodali posebne flourescentne delce PMMA-Rhodamin B, ki zeleno svetlobo (532 nm) odbijajo v rumenem spektru (590 nm).

Tako je bila z uporabo dveh kamer CCD mogoča hkratna določitev hitrostnega polja in

The problem with using the PIV method in cavitation flow is that the present vapour structures reflect too much light so that the acquisition of the information about the velocity field inside the cavity is impossible. A relatively new technique of combining the PIV method with the LIF method was used to obtain the information about the velocity field outside and inside the vapour cavity [10]. For the seeding some special PMMA-Rhodamin B fluorescence particles that reflect the green light (532 nm) in the yellow spectrum (590 nm) were added to the water.

This way it was possible to use two CCD cameras (the first camera captured only light in yellow spec-

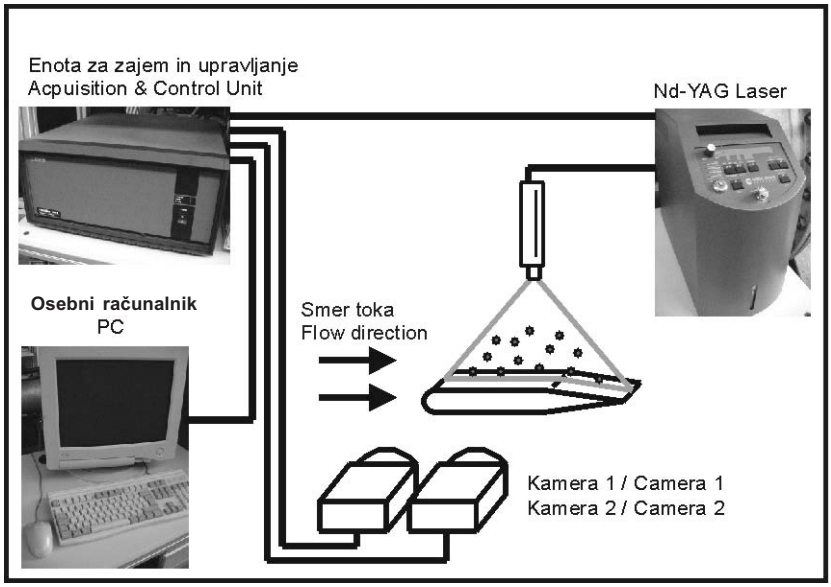

Sl. 3. *Postavitev preizkusa za meritve z metodo PIV-LIF*
Fig. 3. *Experimental setup for measurements with the PIV-LIF method*

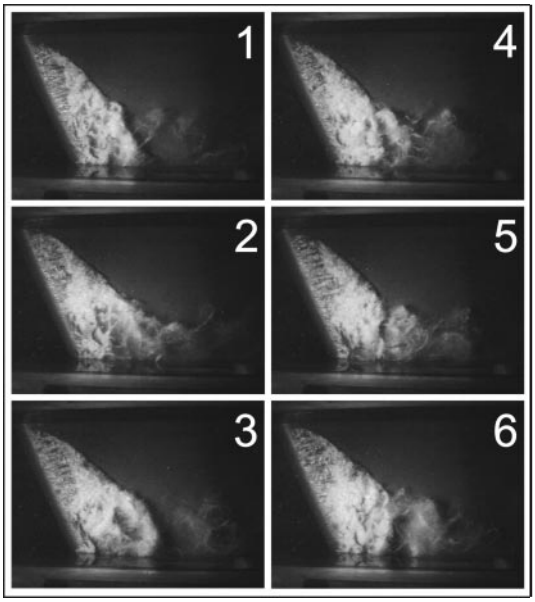

Sl. 4. *Trganje kavitacijskega oblaka nad profilom PNVR pri kavitacijskem številu* $\sigma = 2,0$
Fig. 4. *Cavitation cloud separation on ALE hydrofoil at cavitation number* $\sigma = 2.0$

porazdelitev pare (prva je zajemala samo svetlobo v rumenem spektru in posnela le slike delcev (kavitacijskih struktur na slikah ni mogoče videti), medtem ko je druga zajemala celoten svetlobni spekter in posnela slike kavitacijskih struktur). Da bi dobili informacijo o hitrostnem polju in pripadajoči kavitacijski strukturi na eni sliki, sta bili obe sliki združeni (sl. 5).

Hitrostno polje je bilo določeno samo s pogleda od strani, medtem ko so bile slike kavitacijskih struktur posnete tudi s pogleda od zgoraj (sl. 4) – tok teče z leve proti desni.

Zaporedje na sliki 4 je sestavljeno iz posameznih značilnih slik. Vidimo, da ima kavitacija ob sprednji steni (kjer je profil najkrajši) značilno dinamično obnašanje. Prihaja do trganja kavitacijskega oblaka, ki nato potuje s tokom in izgine v območju z višjim tlakom. Na drugi strani (kjer je profil najdaljši) je kavitacija ustaljena in ne prihaja do trganja oblaka.

Na sliki 5 so prikazana štiri tipična stanja v postopku trganja kavitacijskega oblaka za PNVR pri $\sigma = 2,0$ ter dva povečana detajla. Po odtrganju (1), tik pred odtrganjem (2) in dva primera med samim trganjem (3 in 4). Detajla prikazujeta povratni curek znotraj pritrjene kavitacije (detajl A) in vrtinec za odtrganim kavitacijskim oblakom (detajl B). Tok teče z leve proti desni. Na levih dveh slikah (1 in 2) je mogoče znotraj pritrjene kavitacije opaziti

trum and recorded only the images of the tracer particles (the vapour structure is not visible in the image), while the other captured the whole light spectrum and recorded the image of the vapour cavity to determine the flow field and the distribution of the vapour simultaneously. The two pictures where superimposed to get information about the velocity field and about the dimensions of the vapour cavity in the picture (Fig. 5).

The velocity field was determined only from a side view, while the images of the vapour structures were recorded from the top view also (Fig. 4). In the figure the flow is from left to right.

The sequence is made from characteristic single images. We can see that the cavitation behaves dynamically at the front wall (where the hydrofoil is the shortest). In this region the separation of the cavitation cloud occurs. The separated cloud then travels and implodes in a region with higher pressure. On the other side (where the hydrofoil is the longest) the cavitation is steady (without cloud separation).

Four typical situations in the cavitation cloud separation process and two magnified details of the ALE hydrofoil at $\sigma = 2.0$ are shown in Fig. 5. After the cloud separation (1), just before the cloud separation (2), and two cases during the separation itself (3 and 4). The details show the re-entrant jet inside the attached part of the cavity (detail A) and a vortex behind the separated cavitation cloud (detail B). The flow is from left to right. A significant vortex (re-entrant jet) can be

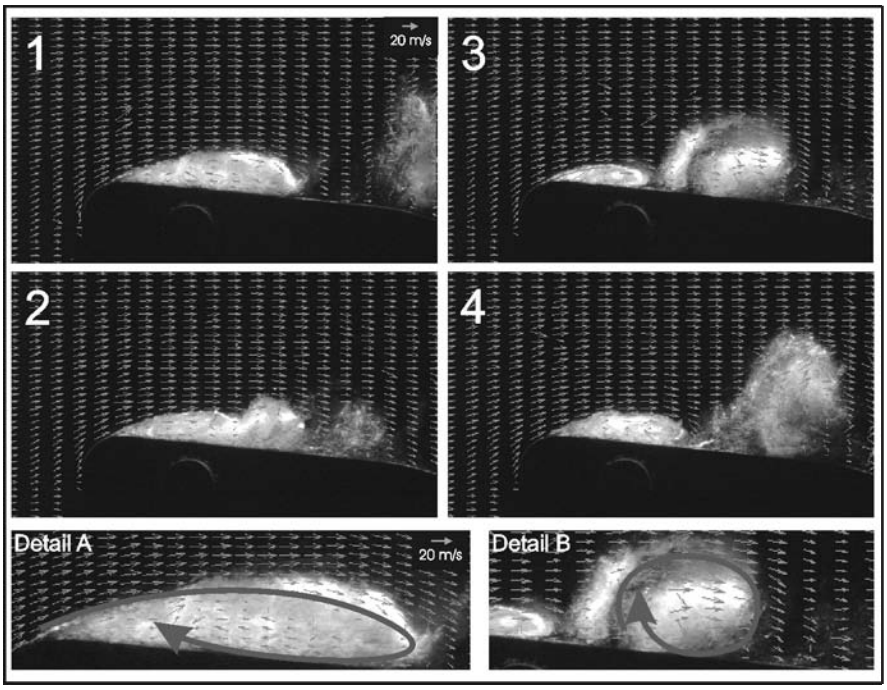

Sl. 5. *Primeri s preizkusi dobljenega hitrostnega polja in kavitacijskih struktur (profil z NVR pri σ = 2,0)*
Fig. 5. *Examples of experimentally obtained flow field and vapour distribution (ALE hydrofoil at σ = 2.0)*

značilen vrtinec (povratni curek). Povratni tok je prisoten od konca kavitacije do 75 % v njeno globino. Z desnih dveh slik (3 in 4) opazimo, da je povratni tok vzrok za trganje kavitacijskega oblaka. Vrtinec ostane znotraj odtrganega oblaka, ki potuje s tokom in izgine v območju z višjim tlakom. Kolaps kavitacijskega oblaka oblikuje nov povratni curek, ki povzroči trganje naslednjega kavitacijskega oblaka.

3 NUMERIČNA SIMULACIJA

Za simulacijo kavitirajočega toka smo uporabili komercialni program Fluent 6.1.18. Program uporablja strukturirane trirazsežne mreže in rešuje sistem časovno odvisnih Reynoldsovo povprečenih Navier-Stokesovih enačb (RPNSE-URANS). Numerični model uporablja posredno metodo končnih prostornin, zasnovan na algoritmu SIMPLE v povezavi z večfaznim in kavitacijskim modelom.

3.1 Večfazni model

Uporabljen je bil postopek homogenega toka mešanice. Lastnosti posameznih faz so vključene v lastnosti enofazne mešanice. Gostota (en. 2) in

seen inside the attached part of the cavitation on the left two pictures. The back flow is detectable from the cavity closure up to 75 % of its length. It can be seen from the right two pictures (3 and 4) that it causes the separation of the cavitation cloud. The vortex remains present inside the separated cloud, which travels with the flow and collapses in the region with higher pressure. The cavitation-cloud collapse forms a new re-entrant jet, which causes a new cloud separation and the process is repeated.

3 NUMERICAL SIMULATION

The commercial code Fluent 6.1.18 was used to calculate the cavitating flow. It is a 3D structured mesh code that solves time-dependent Reynolds-averaged Navier-Stokes equations (URANS). The numerical model uses an implicit finite-volume scheme, based on a SIMPLE algorithm, associated with the multiphase and cavitation model.

3.1 Multiphase model

A single-fluid (mixture phase) approach was used. The properties of the individual phases are included in the single-mixture phase properties. The

viskoznost (en. 3) mešanice sta definirani s prostorninskim deležem pare v mešanici α :

density (Eq. 2) and viscosity (Eq. 3) of the mixture are defined with the volume fraction α:

$$\rho_m = \alpha\rho_v + (1-\alpha)\rho_l \tag{2}$$

in

and

$$\mu_m = \alpha\mu_v + (1-\alpha)\mu_l \tag{3}.$$

Program rešuje kontinuitetno enačbo (4) in gibalno enačbo (5) za tok mešanice (indeks m) skupaj z enačbo prostorninskega deleža (en. 6) za drugo fazo (indeks k):

The continuity (Eq. 4) and momentum (Eq. 5) equations for the mixture flow (index m) together with the volume-fraction equation (Eq. 6) for the secondary phase (index k) are solved:

$$\frac{\partial}{\partial t}\left(\rho_m\right) + \nabla\cdot\left(\rho_m\vec{v}_m\right) = 0 \tag{4}$$

$$\frac{\partial}{\partial t}\left(\rho_m\vec{v}_m\right) + \nabla\cdot\left(\rho_m\vec{v}_m\vec{v}_m\right) = -\nabla p + \nabla\cdot\left[\mu_m\left(\nabla\vec{v}_m + \nabla\vec{v}_m^T\right)\right] + \rho_m\vec{g} + \vec{F} \tag{5}$$

$$\frac{\partial}{\partial t}\left(\alpha_k\rho_k\right) + \nabla\left(\alpha_k\rho_k\vec{v}_m\right) = \dot{m} \tag{6}.$$

3.2 Turbulentni model

Za reševanje prenosnih enačb turbulentne kinetične energije in njene trosilne hitrosti je bil uporabljen turbulentni model RNG k-ε.

Rezultati simulacije, pri kateri smo uporabili običajni turbulentni model RNG k-ε se niso ujemali z eksperimentalnimi rezultati. Pomembnega povratnega toka, ki smo ga opazovali pri preizkusu ni bilo moč simulirati. Poleg tega je bila povprečna dolžina kavitacijske strukture vzdolž profila glede na preizkus za približno 50 odstotkov premajhna. Z namenom, da bi izboljšali simulacijo, smo spremenili člen turbulentne viskoznosti [9]. V območju z velikim deležem pare (majhne gostote mešanice) smo turbulentni model RNG k-ε spremenili z zmanjšanjem turbulentne viskoznosti mešanice (sl. 6):

3.2 Turbulence model

The RNG k-ε turbulence model was applied for solving the transport equations of the turbulent kinetic energy and its dissipation rate.

The results acquired with the use of the standard RNG k-ε turbulence model did not agree well with the experimental results. A significant backflow and cavitation-cloud separation seen during the experiments could not be simulated. Also, the mean cavity-structure length along the hydrofoil was about 50% too small. To improve the simulation a modification of the turbulent viscosity was applied [9]. In regions with higher vapour-volume fractions (lower mixture densities) a modification of the RNG k-ε turbulence model was made by reducing the turbulent viscosity of the mixture (Fig. 6):

$$\mu_t = f\left(\rho\right)\cdot C_\mu\cdot\frac{k^2}{\varepsilon} \tag{7}$$

$$f\left(\rho\right) = \rho_v + \frac{\left(\rho_m-\rho_v\right)^n}{\left(\rho_l-\rho_v\right)^{n-1}} \quad \text{kjer je / where} \quad n >> 1 \tag{8}.$$

Sprememba omeji kinetično energijo in zaradi tega omogoči nastanek povratnega curka ter trganje kavitacijskega oblaka.

This modification limits the kinetic energy and consequently allows the formation of a re-entrant jet and the cavitation-cloud separation.

3.3 Kavitacijski model

Masni delež pare je podan s prenosno enačbo:

3.3 Cavitation model

The vapour mass fraction is given by the transport equation:

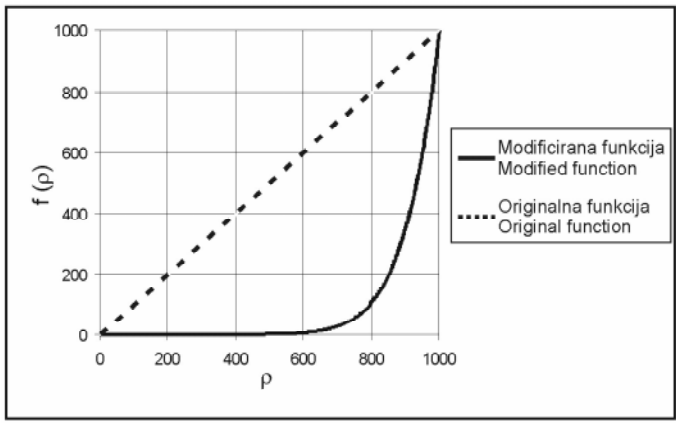

Sl. 6. *Sprememba turbulentne viskoznosti*
Fig. 6. *Modification of the turbulent viscosity*

$$\frac{\partial}{\partial t}\left(\rho_m f\right)+\nabla\cdot\left(\rho_m \vec{v}_m f\right)=R_e-R_c \tag{9}.$$

Izvirna člena R_e in R_c podajata nastajanje (uparjanje kapljevine) in kondenzacijo pare. Člena sta funkciji lokalnih razmer v toku (statičnega tlaka, hitrosti) in lastnosti tekočin (gostot kapljevine in pare, uparjalnega tlaka, površinske napetosti). Izpeljava členov je podana v [3].

Izvorna člena sta podana z:

$$R_e=C_e\cdot\frac{\sqrt{k}}{\gamma}\cdot\rho_l\cdot\rho_v\cdot\sqrt{\frac{2}{3}\cdot\frac{\left(p_v-p\right)}{\rho_l}}\cdot\left(1-f_v-f_g\right)\ ;\qquad \text{pri / when}\quad p<p_v \tag{10}$$

- in z:

$$R_c=C_c\cdot\frac{\sqrt{k}}{\gamma}\cdot\rho_l\cdot\rho_l\cdot\sqrt{\frac{2}{3}\cdot\frac{\left(p-p_v\right)}{\rho_l}}\cdot f_v\ ;\qquad \text{pri / when}\quad p>p_v \tag{11}.$$

kjer sta C_e in C_c empirični stalnici, k lokalna kinetična energija, γ površinska napetost, f_v masni delež pare, f_l masni delež kapljevine in f_g masni delež plinov v vodi.

4 SIMULACIJA IN REZULTATI

Preizkušeni so bili različni tipi in gostote mrež. Nazadnje je bila uporabljena strukturirana mreža tipa C s približno 360000 vozlišči. Ker so bile uporabljene običajne stenske funkcije, je vrednost y^+ ležala med 30 in 80. Za konvergirano rešitev posameznega koraka smo vzeli stanje, ko so ostanki znašali manj ko $5*10^{-4}$. Za konvergirano rešitev posameznega časovnega koraka je bilo potrebnih približno 40 iteracij. Pogoji, pri katerih smo izvajali simulacije, so naslednji:

Source terms R_e and R_c define the vapour generation (liquid evaporation) and the vapour condensation, respectively. The source terms are functions of the local flow conditions (static pressure, velocity) and the fluid properties (liquid and vapour phase densities, vapour pressure and surface tension). The derivation of the source terms can be found in [3].
They are given by:

- and by:

where C_e and C_c are empirical constants, k is the local kinetic energy, γ is the surface tension, f_v is the vapour mass fraction, f_l is the liquid mass fraction and f_g is the mass fraction of the gases in the water.

4 SIMULATION AND RESULTS

Different types and resolutions of meshes were tested. A structured C-type mesh with about 360000 nodes was eventually chosen. Standard wall functions were applied, hence the y^+ value lies between 30 and 80. The time-step solution was considered converged when the residuals fell below $5*10^{-4}$. Approximately 40 iterations per time step were needed to obtain a converged solution. The conditions applied for the simulation are the following:

- Robni pogoji: hitrost na vstopu in statični tlak na izstopu. Na začetku simulacije smo predpostavili majhno hitrost toka, pri kateri kavitacije še ni. Hitrost toka smo nato večali, dokler nismo dosegli želenih razmer.
- Ker je bilo kavitacijsko število pri preizkusu določeno na mestu pred profilom, smo morali za določitev numeričnega kavitacijskega števila upoštevati tlačne izgube, ki nastanejo v testnem odseku. Želene razmere (kavitacijsko število) smo dosegli iterativno s primerjavo eksperimentalnega in numeričnega tlaka na mestu pred profilom.
- Preizkusili smo več dolžin časovnega koraka; na koncu smo uporabili korak dolg $2*10^{-5}$ s.
- Čeprav lahko mešanica pare in kapljevine doseže zvočno hitrost že pri razmeroma majhnih hitrostih, so bili učinki stisljivosti, zaradi poenostvitve simulacije in zmanjšanja računskega časa, zanemarjeni.

4.1 Profil s PVR

Na sliki 7 so prikazane trenutne porazdelitve prostorninskega deleža pare skupaj s pripadajočim hitrostnim poljem. Tok teče z leve proti desni. Kakor na sliki 5 so prikazani štirje primeri (po odtrganju

- Boundary condition: Imposed velocity at inlet and static pressure at outlet. Initial transient treatment: A low velocity is initially applied to the flow field, for which no vapour appears. The velocity is then increased until the considered operating point is reached.
- Because the experimental cavitation number is based on upstream pressure, the losses generated in the test section have to be taken into account in the calculation of the numerical cavitation number. The desired operating point (cavitation number) is reached by comparing the experimental and numerical upstream pressures.
- Different time-step values were tested; eventually a time step of $2*10^{-5}$ s was used.
- Although the vapour-fluid mixture flow can reach the speed of sound at relatively low velocities, compressibility effects were neglected in order to simplify the calculation and decrease the computational time.

4.1 CLE hydrofoil

The instantaneous vapour volume fraction distributions together with the velocity field are shown in Fig. 7. The flow is from left to right. Four cases and two details are shown (like in Fig. 5 – after the cloud separa-

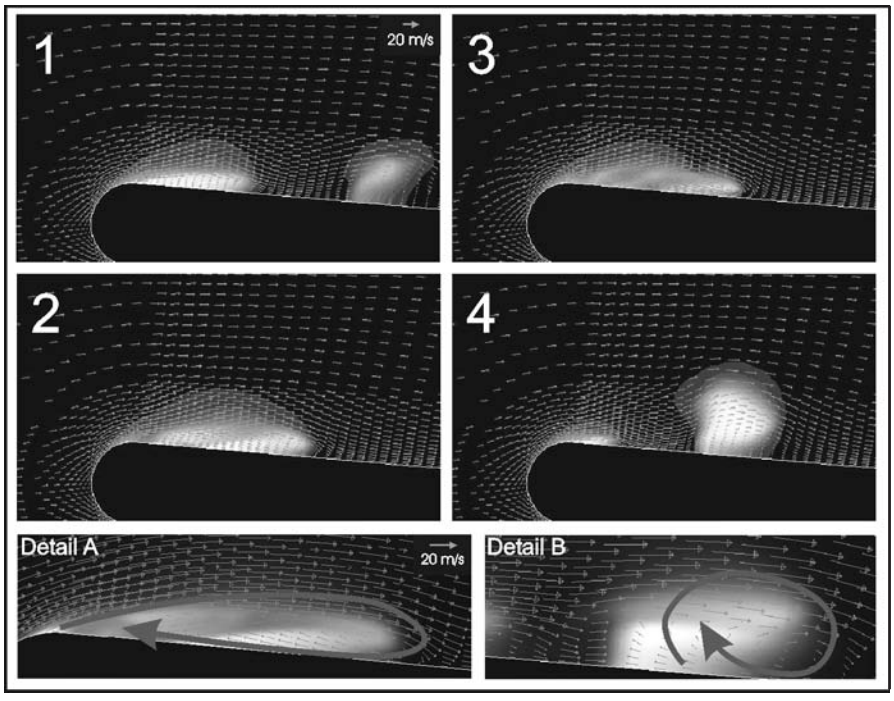

Sl. 7. *Primeri numerične napovedi hitrostnega polja in porazdelitve pare (profil s PVR pri σ = 2,0)*
Fig. 7. *Examples of numerically predicted flow and vapour field (CLE hydrofoil at σ = 2.0)*

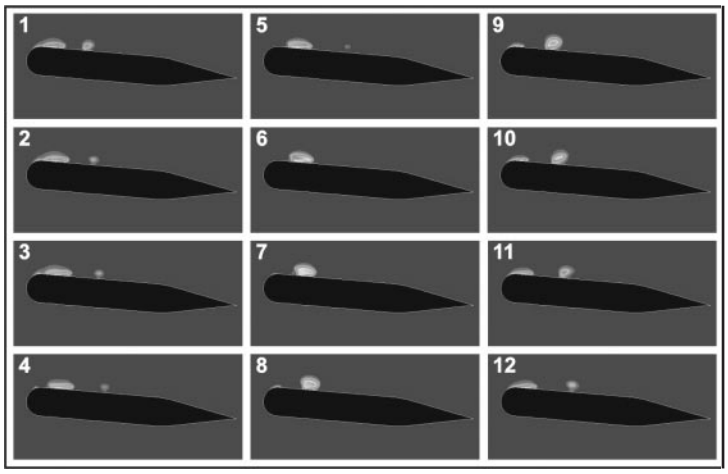

Sl. 8. *Zaporedje trenutnih porazdelitev prostorninskega deleža pare pri σ = 2,5 (pogled od strani)*
Fig. 8. *Sequence of instantaneous vapour volume-fraction distributions at σ = 2.5 (side view)*

oblaka (1), tik pred odtrganjem oblaka (2) ter dve stanji med trganjem oblaka (3 in 4)) ter dva detajla. Pred odtrganjem oblaka (leva spodnja sličica) lahko vidimo vrtinec (povratni curek). Povratni tok, ki je znotraj pritrjene kavitacije, zasledimo do 75 % v njeni globini. V stanju po odtrganju kavitacijskega oblaka lahko razločimo dva vrtinca. Prvega znotraj pritrjene kavitacije (povratni curek), drugega pa nekoliko za odtrganim kavitacijskim oblakom (nastajajoči povratni curek).

Očitno je, da se v vseh primerih numerično napovedano hitrostno polje dobro ujema s preizkusnimi rezultati (sl. 5, 7).

Na sliki 8 vidimo zaporedje trenutnih porazdelitev prostorninskega deleža pare za profil s PVR pri kavitacijskem številu 2,5. Tok teče z leve proti desni. Časovni korak med sličicami je 0,4 ms. Vidimo, da se pritrjena kavitacija zvečuje, dokler se ne odtrga kavitacijski oblak. Pritrjena kavitacija se nato sprva manjša, odtrgani oblak pa potuje s tokom in izgine v območju z višjim tlakom. Med tem se začne pritrjena kavitacija zopet večati in postopek se ponovi.

Med preizkusom smo lahko opazili značilne podkvaste kavitacijske strukture. Na sliki 9 vidimo dve s preizkusi posneti (levo) in numerično napovedani (desno) kavitacijski strukturi. Tok teče z leve proti desni.

4.3 Profil z NVR

Narejena je bila trirazsežna simulacija kavitacije na profilu s poševnim vpadnim robom. Na

tion (1), just before cavitation-cloud separation (2) and two pictures showing the situation during the separation itself (3 and 4)). A single vortex (re-entrant jet) can be seen in the case before cloud separation (bottom-left picture). The back flow is present only inside the vapour cavity. It penetrates the cavity up to 75% of its length. In the case after the cloud separation, two vortices can be determined. One inside the attached vapour cavity (re-entrant jet) and the other one downstream of the separated cavitation cloud (forming the re-entrant jet).

It is obvious that in all cases the numerically predicted velocity field shows a good correlation with the experimental results (Fig. 5 and 7).

A sequence of instantaneous vapour volume fraction distributions for the CLE hydrofoil at cavitation number 2.5 is shown in Fig 8. Flow is from left to right. The time delay between two successive images is 0.4 ms. It is clear that the attached cavitation first grows, until the separation of a cavitation cloud occurs. The attached cavitation part then decreases while the cavitation cloud travels with the flow and collapses in a higher pressure region. Meanwhile, the attached cavitation starts to grow again and the process is repeated.

A typical “horseshoe” vapour structure could be observed during the experiment. Fig. 9 shows two experimentally recorded (left) and numerically predicted (right) cavitation structures. The flow is from left to right.

4.3 ALE hydrofoil

A 3-dimensional simulation of cavitating flow around a hydrofoil with an asymmetric leading

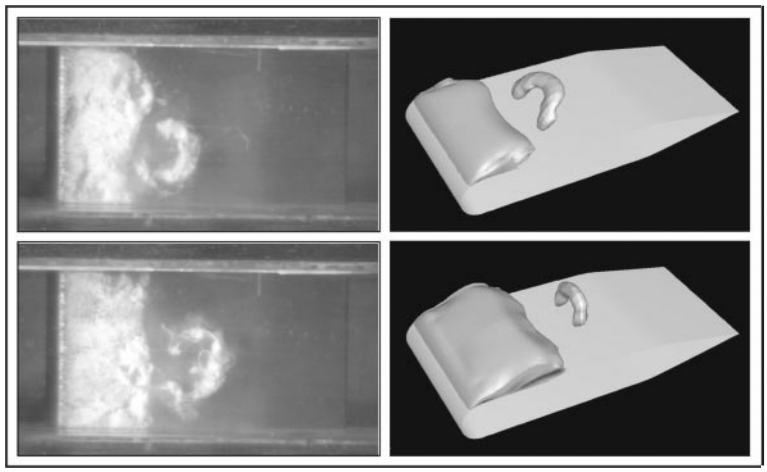

Sl. 9. *Eksperimentalni posnetek (levo) in numerična napoved (desno) podkvaste kavitacijske strukture*
Fig. 9. *Experimental image (left) and numerical prediction (right) of the "horseshoe" cavitation structure*

sliki 10 vidimo trenutne poglede na izopovršino z vrednostjo 0,1 prostorninskega deleža pare. Tok teče z leve proti desni. Časovni korak med sličicami je 0,6 ms. Podobno kakor pri preizkusu [10] vidimo v območju blizu prednje stene očitno dinamično obnašanje kavitacije (utripi kavitacije s trganjem kavitacijskega oblaka). Ob zadnji steni ostaja kavitacija ustaljena (brez trganja kavitacijskega oblaka).

4.4 Povprečna dolžina kavitacije

Primerjali smo eksperimentalno izmerjeno in numerično napovedano povprečno

edge was performed. Instantaneous views of the 0.1 vapour volume-fraction isosurface are shown (Fig. 10). The flow is from left to right. The time delay between successive images is 0.6 ms. Similar to the experiment [10] a significant dynamic cavitation behaviour can be seen near the front wall (pulsations of the cavitation region with the separation of a cavitation cloud), while the cavitation at the rear wall remains steady (with no cloud separation).

4.4 The mean cavity length

The experimentally measured mean cavity structure length along the hydrofoil was compared to the

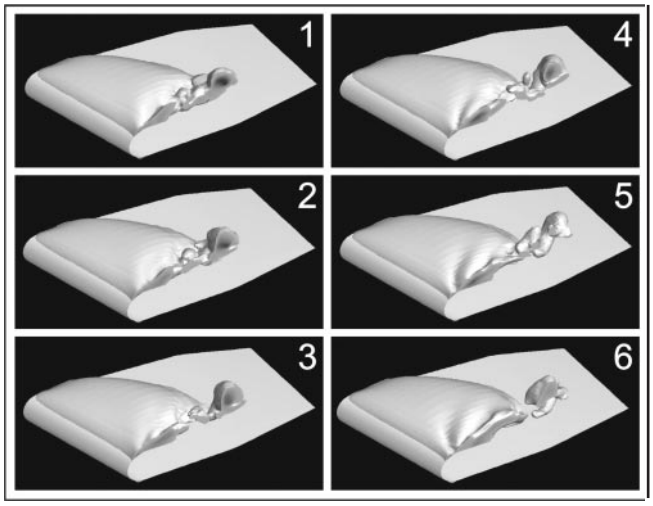

Sl. 10. *Numerično napovedan časovni razvoj kavitacijske strukture pri* $\sigma = 2,0$
Fig. 10. *Numerically predicted time evolution of the cavitation structure at* $\sigma = 2.0$

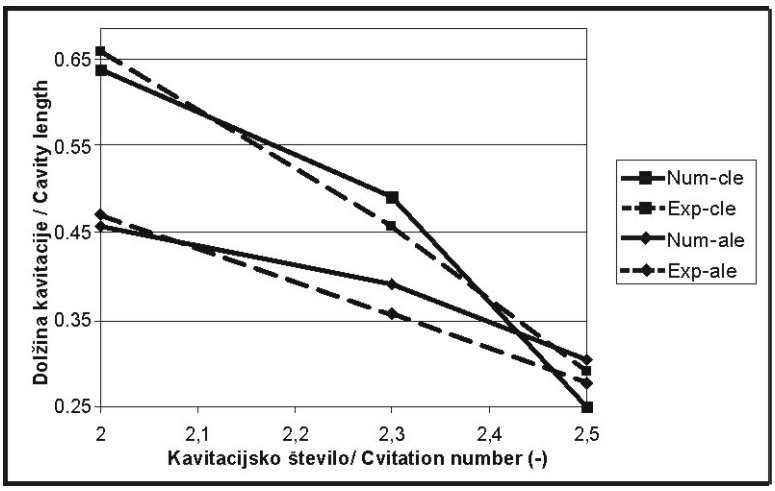

Sl. 11. *Numerično napovedana in s preizkusi določena povprečna dolžina kavitacije*
Fig. 11. *Numerically predicted and experimentally determined mean cavity length*

dolžino kavitacijske strukture vzdolž profila (sl. 11). Povprečno kavitacijsko strukturo smo določili s povprečenjem 50 trenutnih slik kavitacije. Za profil s PVR smo dolžino določili na sredini profila, za profil z NVR pa na mestu laserske ravnine (5 mm od sprednje stene – kjer je profil najkrajši).

Rezultati kažejo, da se povprečna dolžina kavitacije povečuje, ko manjšamo kavitacijsko število. Odvisnost je pri numerični simulaciji pravilno napovedana. Glede na to, da je določanje povprečne velikosti kavitacijske strukture (eksperimentalne ali numerične) razmeroma nenatančno, so rezultati numerične simulacije sprejemljivi.

4.5 Dinamično obnašanje kavitacije

Na sliki 12 so prikazani eksperimentalni in numerični rezultati vrednosti frekvenc trganja kavitacijskega oblaka v različnih razmerah. Eksperimentalne vrednosti frekvenc trganja za profil s PVR smo dobili s prejšnjih meritev dinamičnih tlakov na površini profila ([11] in [12]). Frekvence trganja za profil z NVR smo dobili s filmov, ki smo jih posneli s hitro kamero (približno 2800 sličic na sekundo). Merili smo frekvence za različna kavitacijska števila med 1,8 in 2,7. Numerične frekvence trganja smo izračunali iz simulacije v trajanju približno 10 ponovitev.

Vidimo (sl. 12), da imajo numerično napovedane in s preizkusi določene frekvence trganja enak značaj. Frekvenca trganja se manjša, ko manjšamo kavitacijsko število. V primeru profila s PVR so napovedi frekvence nekoliko previsoke,

numerically predicted one (Fig. 11). The mean cavitation structure was determined by averaging 50 instantaneous images of the cavitation. For the CLE hydrofoil the length was determined in the middle of the hydrofoil, while for the ALE hydrofoil the length corresponds to the position of the laser light plane (5 mm from the front wall – where the hydrofoil is the shortest).

The results show that the mean cavity length grows when the cavitation number is decreased. The trend is correctly predicted in the numerical simulation. Since the determination of the boundary of the mean cavitation structure (experimental or simulated) is relatively inaccurate, the results of numerical simulation are acceptable.

4.5 The dynamic behaviour of cavitation

Experimental and numerical values for vapour-cloud shedding frequencies for different operating conditions are presented in Fig. 12. The experimental shedding frequencies for the CLE hydrofoil were obtained from similar past measurements of the dynamic pressures on the surface of the hydrofoils ([11] and [12]). The shedding frequencies for the ALE hydrofoil were deduced from the images of a high-speed movie (approximately 2800 fps). Frequencies for different cavitation numbers from 1.8 to 2.7 were measured. The numerical frequencies were deduced from a simulation of about 10 cycles.

It can be seen (Fig. 12) that the numerically predicted and experimental shedding frequencies show the same trend. The shedding frequency decreases when the cavitation number is decreased. In the case of the CLE hydrofoil the predicted frequencies are a little higher,

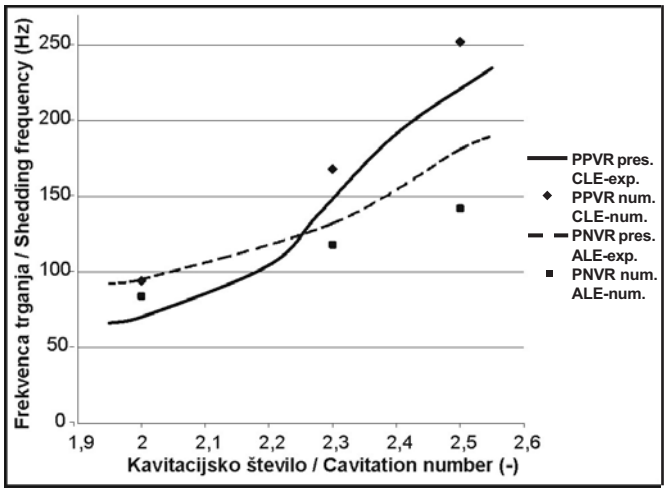

Sl. 12. *Eksperimentalne in numerične frekvence trganja kavitacijskega oblaka*
Fig. 12. *Experimental and numerical shedding frequencies*

v primeru profila z NVR pa nekoliko manjše. Frekvence trganja niso popolnoma nespremenljive. Nihanja v vrednosti lahko ocenimo na +/- 10 % od srednje vrednosti za profil s PVR in +/- 18 % za profil z NVR. Ker je dinamika kavitacije postopek, ki je za simulacijo zelo zahteven, imamo lahko simulacijo za sprejemljivo, če so simulirane in eksperimantalne frekvence trganja enakega velikostnega reda.

5 SKLEPI

Narejeni sta bili numerična in eksperimantalna študija kavitirajočih tokov v različnih razmerah na dveh različnih profilih.

Posneli smo slike kavitacijskih struktur in določili povprečne dolžine kavitacije. Z uporabo razmeroma nove metode PIV-LIF nam je uspelo določiti hitrostno polje zunaj in znotraj kavitacije. S filmov, ki smo jih posneli s hitro kamero, smo določili frekvence trganja kavitacijskih oblakov.

Za simulacijo kavitacije smo uporabili tržni program za računalniško dinamiko tekočin Fluent 6.1.18. Rezultati numerične simulacije kažejo dobro ujemanje z eksperimentalnimi meritvami. Oblike kavitacijskih struktur (na primer podkvasta struktura) so bile pravilno napovedane. Napovedane povprečne dolžine kavitacije se razmeroma dobro ujemajo z eksperimentalno določenimi. Hitrostno polje znotraj kavitacije in zunaj nje je zelo dobro simulirano. Pravilno je napovedan povratni curek, ki povzroči trganje kavitacijskega oblaka. Prav tako

while for the ALE case the predicted frequencies are lower. The shedding frequencies are not perfectly constant. Fluctuations can be estimated in a range of +/- 10 % from the mean value for the CLE hydrofoil and +/- 18 % for the ALE hydrofoil. Cavitation dynamics is a particularly complicated process to simulate. The simulation is considered acceptable if numerically simulated shedding frequencies are of the same order of magnitude as the experimentally obtained ones.

5 CONCLUSIONS

Numerical and experimental investigations of different cavitating flow conditions on two different hydrofoils were performed.

Images of the cavitation structures were recorded and the mean cavitation lengths were determined. With the use of a relatively new PIV-LIF method we were able to determine the velocity fields outside and inside cavitation. From films that were recorded by high-speed camera the cavitation-cloud shedding frequencies were determined.

A commercial CFD program, Fluent 6.1.18, was used for the simulation of the cavitation. The results of the numerical simulation show a good correlation with the experimental measurements. The shapes of the cavitation structures (for example, the "horseshoe" shape) were correctly predicted. The predicted mean lengths of the cavities agree relatively well with the experiment. The velocity fields inside and outside the vapour cavity are particularly well simulated. The backflow phenomenon that causes cavitation-cloud separation was correctly predicted. The simulation also shows good

simulacija dobro napove dinamično obnašanje kavitacijskih oblakov. Simulirane frekvence trganja kavitacijskih oblakov so za primer profila s PVR nekoliko višje za primer profila z NVR pa nekoliko nižje od eksperimetalno določenih.

Naslednji korak je izboljšava simulacije z upoštevanjem učinkov stisljivosti. Izziv je tudi zmanjšanje računskega časa simulacije, ki je presegal 300 ur na osebnem računalniku s procesorjem Pentium IV – 2,4 GHz (glej [13]).

Predstavljeni rezultati obetajo možnost napovedi dinamičnih učinkov kavitacije, na primer kavitacijske erozije, z izključno numeričnimi orodji.

prediction of the dynamic behaviour of cloud cavitation. The simulated frequencies of vapour-cloud shedding are generally a bit higher than the experimentally obtained ones for the CLE hydrofoil and lower for the ALE hydrofoil.

The next step is to upgrade the simulation by considering the compressibility effects. Another challenge is to reduce the computational time, which exceeded 300 hours for a simulation using a Pentium IV – 2.4 GHz processor [13].

The presented results promise the possibility of the prediction of dynamic cavitation effects, like cavitation erosion, using only CFD.

6 SIMBOLI
6 NOMENCLATURE

empirična konstanta	C_e	-	empirical constant
empirična konstanta	C_c	-	empirical constant
sila	F	N	force
masni delež	f	-	mass fraction
masni delež pare	f_v	-	vapour mass fraction
masni delež plinov	f_g	-	gas mass fraction
težnostni pospešek	g	m/s^2	gravitational acceleration
turbulentna kinetična energija	k	m^2/s^2	turbulence kinetic energy
masni tok	m	kg/s	mass flow
tlak	p	Pa	pressure
tlak uparjanja	p_v	Pa	vapour pressure
hitrost mešanice	v_m	m/s	mixture velocity
hitrost k-te faze	v_k	m/s	k-th phase velocity
prostorninski delež *k*-te faze	α_k	-	k-th phase volume fraction
disipacijska hitrost turbulence	ε	m^2/s^3	turbulence dissipation rate
površinska napetost	γ	N/m	surface tension
viskoznost mešanice	μ_m	Pa s	mixture viscosity
gostota kapljevine	ρ_l	kg/m^3	liquid density
gostota *k*-te faze	ρ_k	kg/m^3	k-th phase density
gostota mešanice	ρ_m	kg/m^3	mixture density
gostota pare	ρ_v	kg/m^3	vapour density
kavitacijsko število	σ	-	cavitation number

7 LITERATURA
7 REFERENCES

[1] Širok, B., M. Dular, M. Novak, M. Hocevar, B. Stoffel, G. Ludwig, B. Bachert (2002) The influence of cavitation structures on the erosion of a symmetrical hydrofoil in a cavitation tunnel; *Journal of Mechanical Engineering*, vol. 48, no. 7, Ljubljana, Slovenia.

[2] Kubota, A., H. Kato, H. Yamaguchi (1992) A new modelling of cavitating flows: A numerical study of unsteady cavitation on a hydrofoil section; *Journal of Fluid Mechanics*, vol. 240, 59-96.

[3] Sauer, J. (2000) Instationär kavitierende Strömungen - Ein neues Modell, basierend auf Front Capturing (VoF) und Blasendynamik – PhD thesis; *Universität Karlsruhe* (TH), Karlsruhe.

[4] Singhal, A.K., Li H., M.M. Atahavale, Y. Jiang Y. (2002) Mathematical basis and validation of the full cavitation model; *Journal of Fluids Engineering*, 124, 617-624.
[5] Dular, M., B. Širok, B. Stoffel, B. Bachert, R. Bachert (2003) Numerical simulation of cavitation on a single hydrofoil in a cavitation tunnel; *Slovensko društvo za mehaniko*, Kuhljevi dnevi, Zreče.
[6] Coutier-Delgosha, O., R. Fortes-Patella, J.L. Reboud (2001) Evaluation of turbulence model influence on the numerical simulations on unsteady cavitation; *Proceedings of ASME FEDSM 01, 2001 ASME Fluids Engineering Division Summer Meeting*, New Orleans, Louisiana, May 29-June 1.
[7] Hofmann, M., H. Lohrberg, G. Ludwig, B. Stoffel, J.-L. Reboud, R. Fortes-Patella (1999) Numerical and experimental investigations on the self - oscillating behaviour of cloud cavitation - Part 1: Visualisation; *Proceedings of the 3rd ASME / JSME Joint Fluids Engineering Conference,* San Francisco CA.
[8] Lohrberg, H., B. Stoffel, R. Fortes-Patella, J.L. Reboud (2001) Numerical and experimental investigations on the cavitation flow in cascade of hydrofoils; *Procedings of the Fourth International Symposium on Cavitation,* California Institute of Technology, Pasadena, California, USA, 20-23 June,
[9] Reboud, J.L., B. Stutz, O. Coutier (1998) Two-phase flow structure of cavitation: experiment and modelling of unsteady effects: *Third International Symposium on Cavitation*, Grenoble, France.
[10] Bachert, R., B. Stoffel, R. Schilling, M. Frobenius (2003) Three-dimensional, unsteady cavitation effects on a single hydrofoil and in a radial pump – Measurements and numerical simulations; Part one: Experiments; *Procedings of the Fifth International Symposium on Cavitation*, Osaka, Japan, November 1-4.
[11] Hofmann, M. (2001) Ein Beitrag zur Verminderung des erosiven Potentials kavitierender Stömungen – PhD thesis; *Technische Universität Darmstadt*, Darmstadt.
[12] Boehm, R. (1998) Erfassung und hydrodynamische Beeinflussung fortgeschrittener Kavitationszustände und ihrer erosiven Aggressivität – PhD Thesis; *Technische Universität Darmstadt,* Darmstadt.
[13] Frobenius, M., R. Schilling, R. Bachert, B. Stoffel (2003) Three-dimensional, unsteady cavitation effects on a single hydrofoil and in a radial pump – Measurements and numerical simulations; Part two: Numerical simulation*; Proceedings of the Fifth International Symposium on Cavitation*, Osaka, Japan, November 1-4.

Naslova avtorjev: Matevž Dular
prof.dr. Brane Širok
Univerza v Ljubljani
Fakulteta za strojništvo
Aškerčeva 6
1000 Ljubljana
matevz.dular@fs.uni-lj.si
brane.sirok@fs.uni-lj.si

Rudolf Bachert
prof. dr. Bernd Stoffel
Tehnična univerza Darmstadt
Magdalenenstrasse 4
D-64289 Darmstadt, Nemčija
rbachert@tfa.maschinenbau.tu-darmstadt.de
stoffel@tfa.maschinenbau.tu-darmstadt.de

Authors' Addresses: Matevž Dular
Prof.Dr. Brane Širok
University of Ljubljana
Faculty of Mechanical Eng.
Aškerčeva 6
1000 Ljubljana, Slovenia
matevz.dular@fs.uni-lj.si
brane.sirok@fs.uni-lj.si

Rudolf Bachert
Prof.Dr. Bernd Stoffel
Darmstadt University of Tech.
Magdalenenstrasse 4
D-64289 Darmstadt, Germany
rbachert@tfa.maschinenbau.tu-darmstadt.de
stoffel@tfa.maschinenbau.tu-darmstadt.de

Prejeto: 29.6.2004
Received:
Sprejeto: 2.12.2004
Accepted:
Odprto za diskusijo: 1 leto
Open for discussion: 1 year